



THE EVALUATION OF THE MIXING LAYER FORMATION WHEN SOUND WAVES PROPAGATE THROUGH A MEDIUM WITH HIGH AND LOW OIL CONCENTRATION REGIONS

^{1,2} Neodir José Comunello

¹Instituto Tecnológico de Aeronáutica, Departamento de Propulsão. Pça Mal. Eduardo Gomes, 50
São José dos Campos, SP, Brasil, 12228-900

²Agência Nacional de Aviação Civil, Avenida Cassiano Ricardo, 521

São José dos Campos, SP, Brasil
neodir.comunello@anac.gov.br

Cristiane Aparecida Martins

Instituto Tecnológico de Aeronáutica, Departamento de Propulsão. Pça Mal. Eduardo Gomes, 50
São José dos Campos, SP, Brasil, 12228-900
cmartins@ita.br

Pedro Teixeira Lacava

Instituto Tecnológico de Aeronáutica, Departamento de Propulsão. Pça Mal. Eduardo Gomes, 50
São José dos Campos, SP, Brasil, 12228-900
placava@ita.br

Abstract. This paper presents the evaluation of the physical interpretations related to the generation of mixing layers when separated regions of high and low oil concentration in air is submitted to sound waves. The main hypothesis pursued here is that the acoustic field increases the fuel-air mixing performance and makes the temperature distribution in the flame more uniform, which prevents the formation of nitrogen oxides in the non premixed combustion camera. After experimental observation registered in pictures it is proposed two mechanisms to be the responsible for the mixing layer generation. The first evaluation discarded both, however reevaluating the hypothesis with a better quantification equation it is very likely to indicate the shear flow instability caused by the difference between the acoustic particle velocities in the high and low oil concentration as the responsible for the mixing layers generation. Accepting this mechanism to go on with the investigation it is suggested to solve the rotational part of the acoustic particle velocity that appear in the Stokes-Navier equation, which becomes important near the boundary between high and low oil concentration regions. Additional tests at different input frequencies and instrumentation able to acquire the oil concentration, the acoustic pressure and particle velocity are suggested as well. The results are not exactly quantified, however the qualification obtained clears the role of the wave energy dissipation in the mixing layer generation and can help future works in this research field.

Keywords: combustion, mixing layer formation, fuel-air entrainment, acoustic particle velocity.

1. INTRODUCTION

The mixture process is spontaneous and well established by the diffusion theory. Usually it takes a long time up to reach the desired mixture of the constituents. When this time is not available is usual to force the convection of one constituent against the others to speed up the process. In one combustion system where the fuel and the oxidant are conducted separately it is normal occurs non-uniformity inside of the stream. This non-uniformity will affect the flame structure and possibly the pollutants mechanism. For example, Appleton e Heywood (1972) studied the influence between non-uniformity and NOx formation. They concluded that increasing of the non-uniformity is responsible to one increase of the NOx formation only in lean fuel condition ($\phi < 0.85$). Blevins e Gore (1995) showed as well some relationship between emission NOx and mixture rate. Lyons (1982) did one study which try to relate the degree of non-uniformity and NOx emission. There are another literature studies nevertheless still there doubt about the exact influence between mixture process and combustion process. Also, it is already known that the acoustic field has strong influence during mixture process. This is applied more obviously in non-premixed combustion. However, even in premixed combustion where the reduction of nitrogen oxides, in general, is achieved by lean mixtures, the interaction between the acoustic waves generated by the turbulent flame and the premixed fuel outlet can lead to intolerable levels of acoustic pressure amplitude (Kampen, 2006).

The present work try to better understand the process between acoustic and mixture process. The focus is the application in combustion process. It was did measurements utilizing PIV and the velocity fields with acoustic influence are analyzed to light of the entropy concept. One simple observation is able to show the strong influence of the acoustic field. After was done one mathematic consideration and finally some considerations with conclusions not end until now.

Comunello, N.J., Martins, C.A. and Lacava, P.T.
Mixing Layer Formation Under Sound Wave Motion

2. EXPERIENCE DESCRIPTION

The basic experimental assembly was the same as constructed and reported in the work of Comunello *et al.* (2013). The accretion regarding the experience's installation is one internal tube of 9.52 mm diameter to provide a reach flow of seed particles. It was installed in the pressure plug position 5, the position closest to be loudspeaker, and connected directly with the seeder; as illustrated in "Fig. 1".

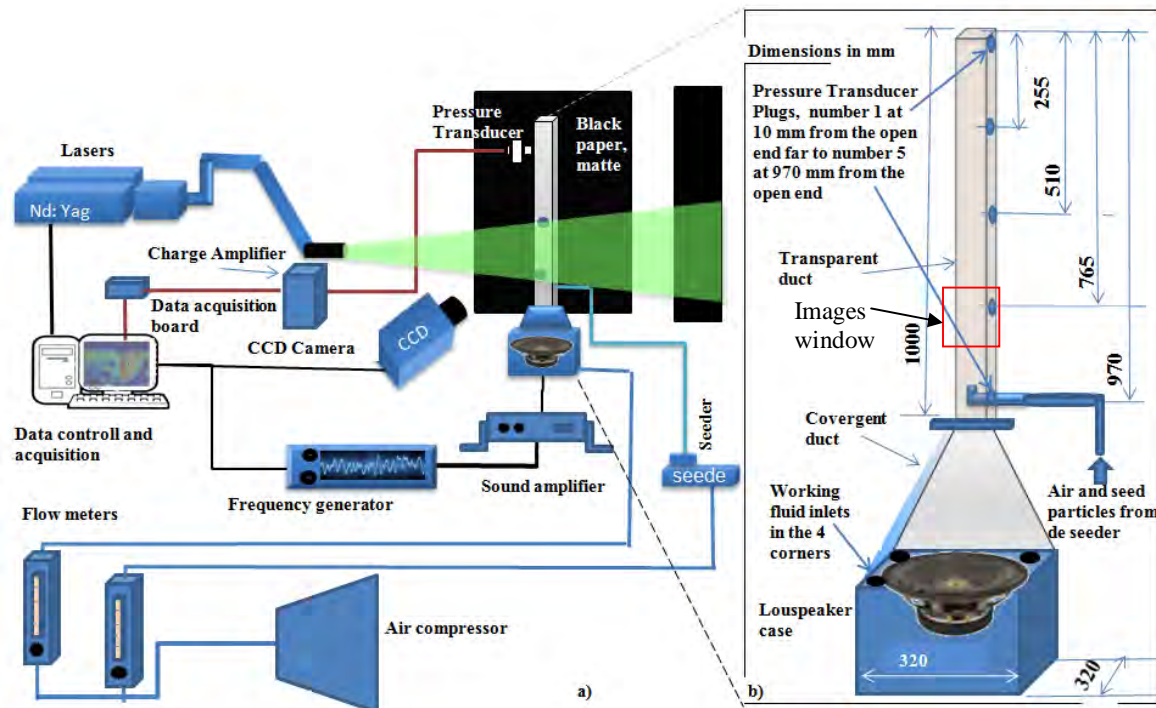


Figure 1. a) General assembly with a modification in the seeder line and b) additional inner tube to provide air with high concentration of the seeder particles and the position where images were captured.

The inner tube enters into the main duct at 970 mm from the duct open end with its outlet aligned with the main duct centerline at 920 mm.

3. METODOLOGY

The experimental procedure was to inject some amount of air with high concentration of seed particle. It was waited few minutes up to the fluid come in rest with enough separation between air and seed particles of mineral oil. The images began to be captured before the sound system was turned on, so the images captured covered the initiation of the mixing process until the complete mixture of air with the seed particles.

The test was performed with input frequencies of 100 Hz and 161 Hz, the last being the assembly resonance frequency. Initially the tests were done for free, just to see if the sound would interact with the mixing process. The observation of the experience through the pictures is the starting baseline, afterwards it is look for possible physical interpretations and theirs mathematical theories, which are followed by the validation, or not, of the interpretations with the observation.

4. OBSERVATIONS

The results presented herein are related to the measures done inside the duct. The center of the images captured is at 800 mm from the duct open end with 80 mm of height.

When the fluid is left to rest only natural convection movement was noticed. The high and low oil concentration regions took the form of a spiral like pattern, however with a small rotational velocity in the counterclockwise direction. This initial condition is showed in “Fig. 2”.

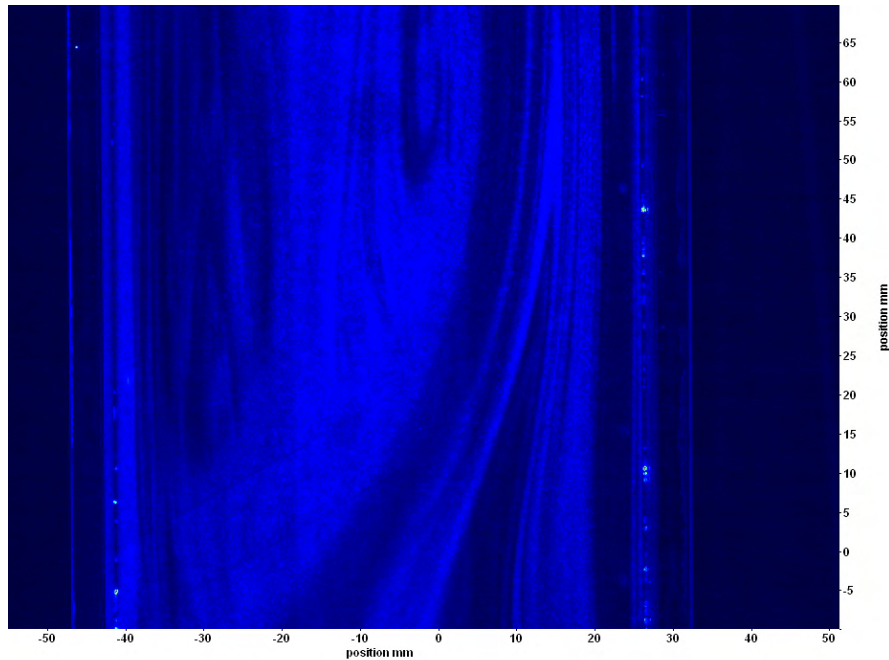


Figure 2. Initial condition of the working fluid

At input frequency of 100 Hz the first image which is noticed the sound action is when all the seed particles were displaced an amount compatible with the acoustical displacement in the position, however without mixing signals. Taking into consideration that the pictures acquisition rate is 14.7 Hz, this means that between two successive images almost 7 acoustic cycles occurred. The subsequent image showed the beginning of a mixing process, it came from the centerline and turned to the right following the high oil concentration path, as showed in the “Fig. 3”.

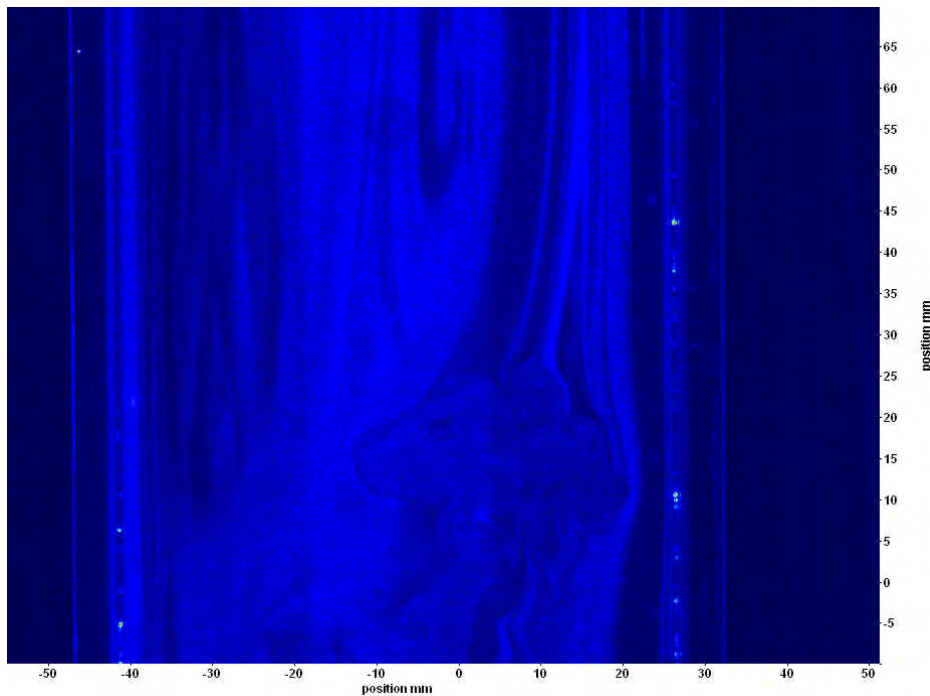


Figure 3. Beginning of the mixing layer due the sound movement ($t = t_0 + 0.136$ s)

Comunello, N.J., Martins, C.A. and Lacava, P.T.
Mixing Layer Formation Under Sound Wave Motion

Where the mixing process took place the form of the observed movements is analogue with the movement of two vortices generated in either border of the high concentration region, with the consequent diffusion of the oil to the low concentration region.

The third and fourth images showed the mixing process going on with an increasing number of vortices, as showed in the “Fig. 4 a) and b)”. The vortices appeared in the border of the high concentration regions as observed in the first movement.

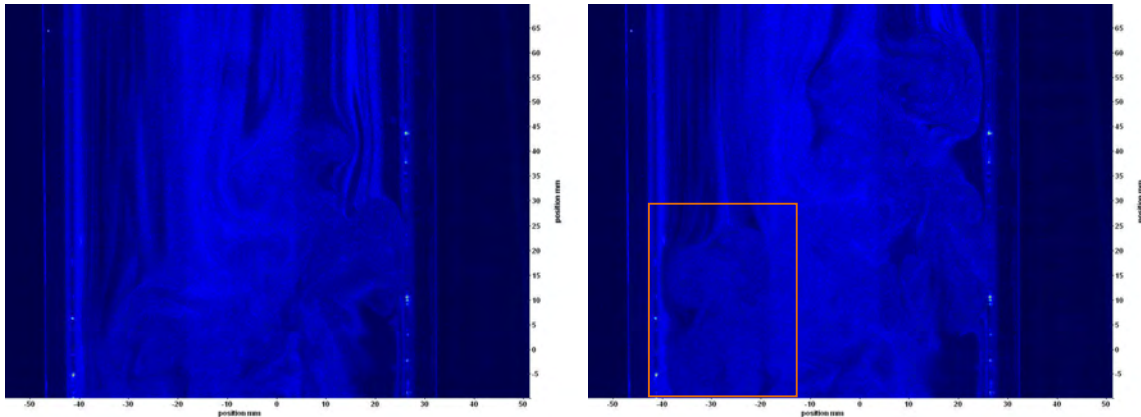


Figure 4. a) Vortices grow their mean vorticity thickness at $t = t_0 + 0.204$ s, b) Other parts of the fluid begins to generate the mixing layer, as the region highlighted with a rectangle frame in the bottom at left of image at $t = t_0 + 0.272$ s.

The end of the mixing process, observed visually in the image's available window, occurred 3.06 seconds later than the moment that the sound was turned on. As showed in “Fig. 5” the high and low concentration regions merged in an almost uniform oil concentration.

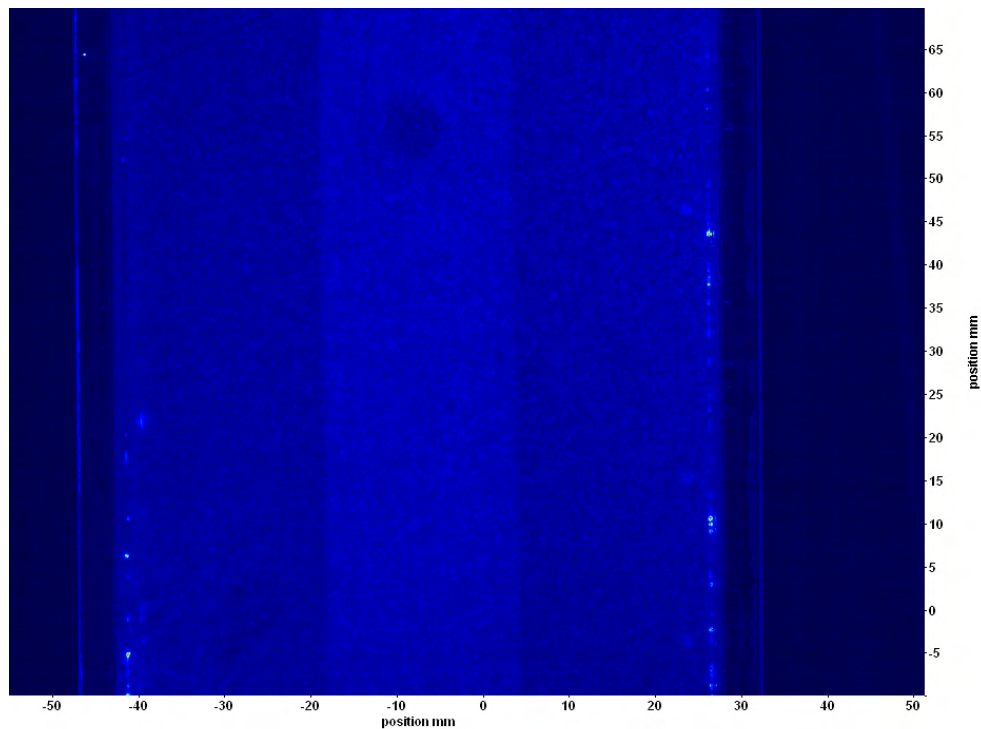


Figure 5. The end of the mixture process, the seed particles concentration is close to uniform overall the image window dimension. The hole in the top-center is the pressure sensor plug number 4 and the white strip in along the centerline is a back support for all the pressure plugs.

At input frequency of 161 Hz the quality of mixing movements are similar those observed at 100 Hz. Since both images set are captured with an acquisition rate of 14.7 Hz, the time between subsequent images is 0.068 seconds. The first picture just show an displacement compatible with the acoustic displacement. Only in the second image, showed in “Fig. 7 a” it is noticed the beginning of a mixing layer, it came from the centerline and twisted the high oil concentration regions.

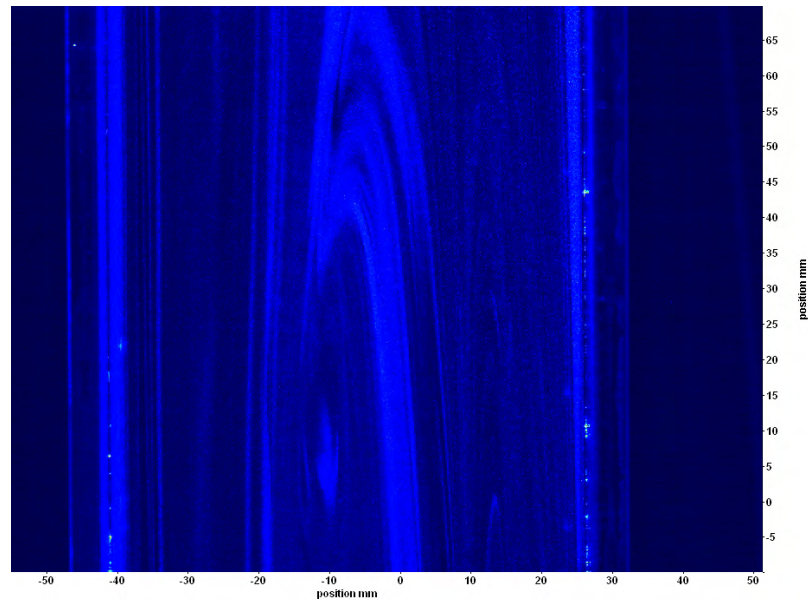


Figure 6. Initial condition of the test with input frequency of 161 Hz

The third image shows the mixing layer expanding laterally, it is clear in the “Fig. 7 b” the increase of the mean vortices thickness and their lateral movement.

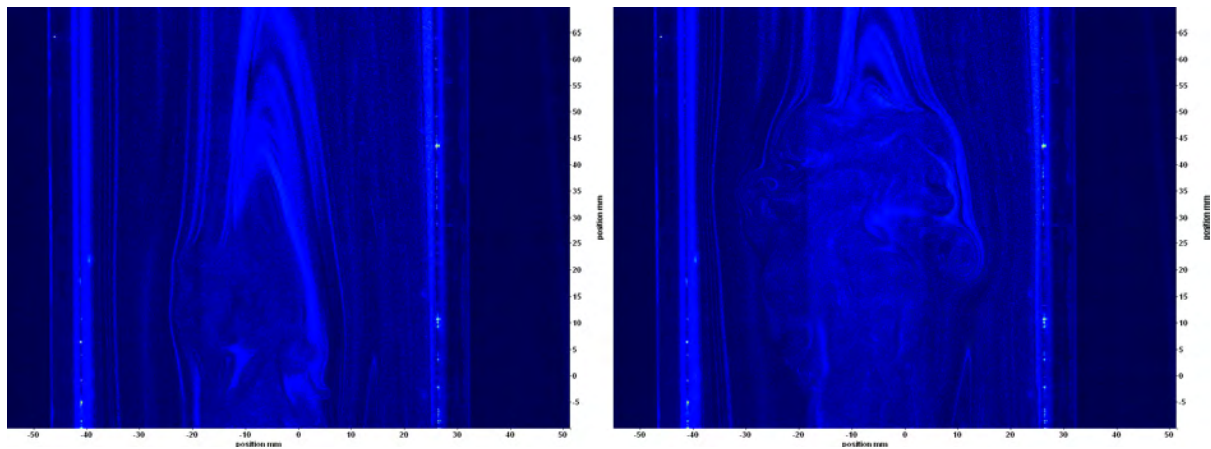


Figure 7. a) Beginning of the mixing layer at $t = t_0 + 0.136$ s and b) development of the mixing layer in width and vorticity at $t = t_0 + 0.204$ s.

It is notable that the grow of the mean vorticity thickness plays a protagonist rule in the spread out of the mixing layers, as showed in “Fig. 8”. Typically at the right side of the high oil concentration layer the vortices rotate in the clockwise direction, while in the left side theirs rotation is in the opposite direction.

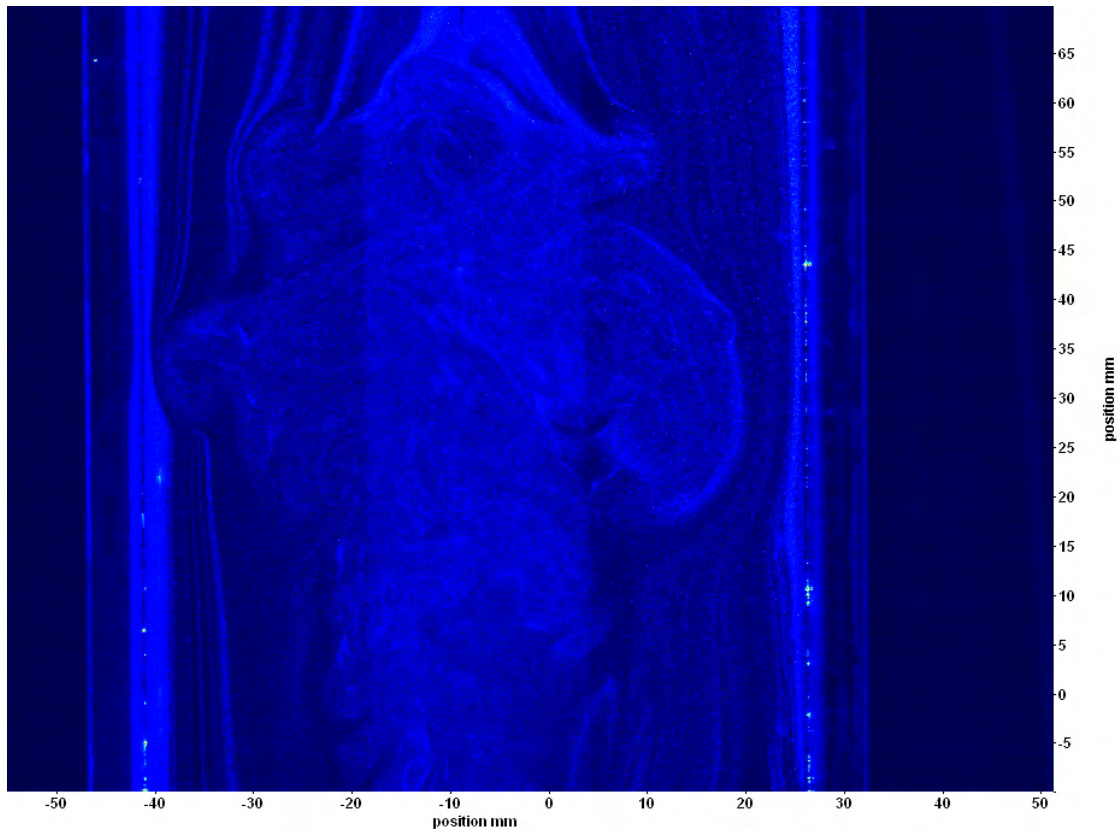


Figure 8. Increase in the mean vorticity thickness with lateral expansion up to reach the duct walls, at $t = t_0 + 0.272$

The first movements at input frequency of 161 Hz are more intense than that observed at input frequency of 100 Hz, however the time to reach a visual homogeneity of the window was about 2 seconds.

5. PHYSICAL INTERPRETATION

5.1 QUALIFICATION

It is visible that the beginning of the mixing movements takes place in the regions of high oil concentration. The oil particles firstly move in normal direction of the borders between low and high oil concentration and then increase in mean vorticity thickness. For sure the energy for these movements comes from the sound wave energy, they are not expected for planar sound waves, except if dissipation is considered. Therefore the oil particles are damping the sound waves energy.

After Chapman and Cowling (1953) and Billet *et al* (2008) it is pointed out and it is shown that the energy dissipation in oscillating movements due the volume viscosity may be greatly increased by small impurities. Hence besides the ordinary viscosity the volume - or bulk- viscosity must be consider in the energy dissipation equation.

So far it is clear that the difference between the sound wave energy losses in the high and low oil concentration is the cause of the mixing layer herein observed. However it is not clear the mechanism developed from the energy dissipation up to reach the mixing layer, the hypothesis are:

a) Development of an instable shear flow in the border between the high and low oil concentration regions: this mechanism is applied to border's surfaces aligned with the sound wave travelling direction and takes account that in the high concentration regions the acoustic pressure and consequently the acoustic particle velocity are strongly attenuated; nevertheless, in the low oil concentration region the acoustic particle velocity suffer less attenuation, consequently its acoustic particle velocity is bigger than the acoustic particle velocity at high oil concentration region. Hence a shear flow takes place in the border between the high and low oil concentration, which generates the mixing layers observed in the images.

b) Development through the difference of temperature between the high and low oil concentration regions due the heating process: this mechanism doesn't depend on the orientation of the border's surface and takes into account that the sound wave energy loss is converted in heat. The wave energy dissipation in the high concentration regions is larger than the energy dissipation in the low oil concentration regions. As observed the onset of the forced convective

movement doesn't take place immediately after the sound waves input. During the firsts cycles of the sound wave, the heating process progresses without volume changes, so the static pressure increases proportionally to the temperature. The pressure increase in the high concentration region will be larger than the pressure increase in the low oil concentration region, with the time goes on the pressures difference increases up to be enough to overcome the superficial tension that maintains the regions apart. Hence a local flow erupts from the high concentration fluid to the low concentration region. Once this flow is initiated the heating process becomes an expansion at constant pressure, where the energy loss from the sound wave acts like a pump to maintain the expansion movement. As soon as a portion of fluid goes out from the high concentration region it is noticed a counterflow on its surroundings from the low concentration fluid to the high concentration region. The local flow and the counterflow on its surroundings gives rise to vortices, similar to those seen in the mixing layers.

Independently of what mechanism is responsible to the development of the mixing layer, or even both, the mixing process actually occurs at molecular scale, so the forced convective movements described above act to enhance the surface contact between high and low oil concentration portions and consequently the improvement of the performance of the mixing process.

The acoustic pressure amplitudes used in the test are in the order of 1000 Pa or about 1% of the ambient pressure; since the pressure amplitude is small compared with the ambient pressure the first-order equation of motion can be used to represent the wave motion. This quality will lead to the familiar wave equations.

The acoustic pressure and consequently the acoustic particle velocity will be considered to maintain the same amplitudes that what measured in a homogenous low oil concentration in the work of Comunello *et al.* (2013).

5.2 QUANTIFICATION

The energy transfer begins with the damping of the wave due to the fluid volume and dynamic shear viscosities. After Morse and Ingard (1968) the rate of energy loss from viscosity in a volume element $dx dy dz$ - \dot{w}_l''' - can be calculated by:

$$\dot{w}_l''' = \left(\eta + \frac{4}{3}\mu\right) \left[\left(\frac{\partial u_x}{\partial x}\right)^2 + \left(\frac{\partial u_y}{\partial y}\right)^2 + \left(\frac{\partial u_z}{\partial z}\right)^2 \right] + \mu \left[\left(\frac{\partial u_x}{\partial y} + \frac{\partial u_y}{\partial x}\right)^2 + \left(\frac{\partial u_x}{\partial z} + \frac{\partial u_z}{\partial x}\right)^2 + \left(\frac{\partial u_y}{\partial z} + \frac{\partial u_z}{\partial y}\right)^2 \right] \quad (1)$$

Where η is the volume viscosity; μ is the dynamic shear viscosity of the fluid and u_i is the velocity component in the $i \in \{x, y, z\}$ direction.

Since the tests were done in plane wave conditions and the "Eq. 1" is too long to be written, it will be applied to represent a harmonic plane wave traveling in the x direction, which is:

$$\dot{w}_l''' = \left(\eta + \frac{4}{3}\mu\right) \left(\frac{\partial u_x}{\partial x}\right)^2 \quad (2)$$

This local energy lost rate per volume can be related to the local entropy generation rate per volume by:

$$S_{ger}'''_{loc} = \frac{\dot{w}_l'''}{T_{ref}} = \frac{1}{T_{ref}} \left(\eta + \frac{4}{3}\mu\right) \left(\frac{\partial u_x}{\partial x}\right)^2 \Leftrightarrow \overline{S_{ger}'''}_{loc} = \frac{1}{T_{ref}} \left(\eta + \frac{4}{3}\mu\right) \overline{\left(\frac{\partial u_x}{\partial x}\right)^2} \quad (3)$$

Where T_{ref} is the reference absolute temperature of the medium, the \Leftrightarrow signal means "if and only if" and the upper bar signal means the time averaged- or root mean square- of the property.

The acoustic particle for a harmonic plane wave moving in x direction can be set as:

$$u_x(x, t) = u'_{max} \cos\left(\frac{2\pi x}{\lambda}\right) \cos wt \quad (4)$$

Where λ is the wavelength and w the wave angular velocity.

The root mean square -rms- of the acoustic velocity is:

$$\overline{u_x(x)} = \frac{u'_{max}}{2} \cos\left(\frac{2\pi x}{\lambda}\right) = u'_{rms} \cos\left(\frac{2\pi x}{\lambda}\right) \quad (5)$$

Where u'_{rms} is the rms amplitude of acoustic velocity in the duct.

Considering the volume integration with a cross section area (A_v) and a characteristic length (X_c), which has its near cross section placed at position x_0 from the origin, then the rms local entropy generation rate is figured out substituting "Eq. 5" in the "Eq. 3", which yields:

Comunello, N.J., Martins, C.A. and Lacava, P.T.
Mixing Layer Formation Under Sound Wave Motion

$$\overline{\dot{S}_{ger}}_{loc} = \frac{1}{T_{ref}} \left(\eta + \frac{4}{3} \mu \right) \iiint_{x_0, y_0, z_0}^{x_0+\chi_c, y_1, z_1} \left(\frac{\partial u_x}{\partial x} \right)^2 \partial x \partial y \partial z = \frac{1}{T_{ref}} \left(\eta + \frac{4}{3} \mu \right) \int_{x_0}^{x_0+\chi_c} \left(\frac{\partial u_x}{\partial x} \right)^2 A_v \partial x = \frac{u'_{rms^2}}{T_{ref}} \left(\frac{2\pi}{\lambda} \right)^2 \left(\eta + \frac{4}{3} \mu \right) A_v \left(\frac{x}{2} + \frac{\lambda}{4\pi} \sin \frac{4\pi x}{\lambda} \right) \Big|_{x_0}^{x_0+\chi_c} = \frac{u'_{rms^2}}{T_{ref}} \left(\frac{2\pi}{\lambda} \right)^2 A_v \left(\eta + \frac{4}{3} \mu \right) \left(\frac{\chi_c}{2} - \frac{\lambda}{4\pi} \sin \frac{2\pi\chi_c}{\lambda} \cos \frac{2\pi(2x_0+\chi_c)}{\lambda} \right) \quad (6)$$

If the wavelength is much longer than the characteristic length then the sine term can be approximated to the angle and the cosine term just keep the position x_0 where the volume is placed, which yields:

$$\overline{\dot{S}_{ger}}_{loc} = \frac{u'_{rms^2}}{T_{ref}} \left(\frac{2\pi}{\lambda} \right)^2 A_v \left(\eta + \frac{4}{3} \mu \right) \left(\frac{\chi_c}{2} - \frac{\chi_c}{2} \cos \frac{4\pi x_0}{\lambda} \right) = \frac{u'_{rms^2}}{T_{ref}} \left(\frac{2\pi}{\lambda} \right)^2 A_v \left(\eta + \frac{4}{3} \mu \right) \chi_c \left(\sin \frac{2\pi x_0}{\lambda} \right)^2 \quad (7)$$

To be prepared to figure out the thermodynamic changes in the volume under consideration it's better to work with the specific rms entropy generation rate, defined by the ratio of rms entropy generation rate to the mass contained in the volume - m_v - which is:

$$\overline{\dot{S}_{ger}}_{loc} = \frac{\overline{\dot{S}_{ger}}_{loc}}{m_v} = \frac{u'_{rms^2}}{\rho_0 T_{ref}} \left(\frac{2\pi}{\lambda} \right)^2 \left(\eta + \frac{4}{3} \mu \right) \left(\sin \frac{2\pi x_0}{\lambda} \right)^2 \quad (8)$$

Where ρ_0 is the averaged density of the fluid.

The quantification related to each one of the hypothesis are:

- a) The wave attenuates as it proceeds, after Morse and Ingard (1968), for a plane wave the attenuation factor is:

$$a \cong \frac{1}{2} \left(\frac{2\pi}{\lambda} \right)^2 \frac{\left(\eta + \frac{4}{3} \mu \right)}{\rho_0 c} \quad (9)$$

Where c is the wave speed in the medium.

The traveling wave will suffer a reduction in the acoustic particle velocity compared with the non attenuated wave. The quantification of the shear flow instability uses the relative magnitude of the destabilizing shear with respect to average advection velocity, after Huerre (2000), with an adequation to oscillatory movement the velocity ratio may be defined by:

$$R'_a = \frac{u'_{rms} - u'_{a rms}}{u'_{rms} + u'_{a rms}} = \frac{1 - e^{-\frac{1}{2} \left(\frac{2\pi}{\lambda} \right)^2 \frac{\left(\eta + \frac{4}{3} \mu \right)}{\rho_0 c} x}}{1 + e^{-\frac{1}{2} \left(\frac{2\pi}{\lambda} \right)^2 \frac{\left(\eta + \frac{4}{3} \mu \right)}{\rho_0 c} x}} \quad (10)$$

Where R'_a is the average acoustic velocity ratio due the wave attenuation, u'_{rms} and $u'_{a rms}$ are the root mean square acoustic particle velocity in the medium with negligible attenuation and the velocity in the high oil concentration region respectively.

- b) The entropy generated due the viscosities of the fluid is converted in heat. For ideal gases this heating process at constant pressure can be calculated by:

$$\overline{\dot{S}_{ger}}_{loc} \Delta t = C_p \ln \frac{T_2}{T_{ref}} \Leftrightarrow \Delta T = T_{ref} \left(e^{\frac{\Delta t \overline{\dot{S}_{ger}}_{loc}}{C_p}} - 1 \right) \quad (11)$$

Where T_2 is the absolute temperature after the heating process, C_p is the specific heat capacity at constant pressure and Δt is the time elapsed since the beginning of the process.

6. RESULTS AND DISCUSSION

The results presented are related to the possible physical interpretations confront with the observations. So it is foreseen that it will work more as a filter to eliminate or promote the hypothesis aroused than generate exactly results.

The test conditions are known with a good reliability due the work of Comunello *et al.* (2013) and can be tabulated by:

Table 1. Test conditions inside the duct

Input Frequency (Hz)	Distance of the center of the observed images from the duct open - x_0 (m)	Root mean square acoustic particle velocity amplitude - u'_{rms} (m/s)	Acoustic particle velocity derivative regarding the traveling direction at observed position - $\delta u' / \delta x$ (1/s)		Squared acoustic velocity derivative $(\delta u' / \delta x)^2$ - (1/s ²)
			Measured	Calculated	Average between measured and calculated
100	0,8	1,4	2,5	2,6	6,5
161	0,8	9,4	16,2	19,6	324

The working fluid properties presented in the “Tab. 2” are estimated; since the exact mineral oil concentration in the high oil concentration region was not measured it will be estimated as 50% oil and 50% air. The low oil concentration region will be considered with a negligible amount of oil.

Table 2. High oil concentration region estimated properties

Volume to dynamic shear viscosity ratio (η/μ)	0.67
Dynamic shear viscosity- μ - (Pa.s)	0.1
Reference temperature (Kelvin)	300
Average density (Kg/m ³)	6
$\eta + 3\mu/4$ (Pa.s)	0.2
Specific heat capacity at constant pressure (KJ/KgK)	1.5

These data give on first approximation of the specific rms entropy generation rate in the high oil density region, using “Eq. 8” its magnitude order for input frequency of 100 Hz is:

$$\overline{\dot{s}_{ger}}_{loc} = \frac{u'_{rms}{}^2}{\rho_0 T_{ref}} \left(\frac{2\pi}{\lambda} \right)^2 \left(\eta + \frac{4}{3}\mu \right) \left(\text{sen} \frac{2\pi x_0}{\lambda} \right)^2 = 0.0007$$

For input frequency of 161 Hz it is:

$$\overline{\dot{s}_{ger}}_{loc} = \frac{u'_{rms}{}^2}{\rho_0 T_{ref}} \left(\frac{2\pi}{\lambda} \right)^2 \left(\eta + \frac{4}{3}\mu \right) \left(\text{sen} \frac{2\pi x_0}{\lambda} \right)^2 = 0.043$$

a) Evaluation of the heating mechanism - taking into consideration that the wave energy is small compared with the volume energy required to heat an amount of mass, allied with a small time interval observed to beginning the fluid motion, which is in the magnitude order of 1 (one) second, the hypothesis of volume heating is the weakest of the possible mechanisms suggested. The temperature increase in the high oil concentration regions per “Eq. 11” is:

$$\Delta T = T_{ref} \left(e^{\Delta t \frac{\overline{\dot{s}_{ger}}_{loc}}{c_p}} - 1 \right) = \begin{cases} 0.14 \text{ for } 100 \text{ Hz} \\ 8.6 \text{ for } 161 \text{ Hz} \end{cases}$$

The increase of temperature for input frequency 100 Hz is negligible, for 161 Hz it is small, by considerable. The second criteria is the observation that the beginning of the movement observed happened after about 0,13 second for both input frequencies, since the heating mechanism showed differences in the order of 100 (one hundred) in the heating rate it is very unlikely that the mixing layers observed can have the heating mechanism as is starting point.

b) Evaluation of the attenuation difference mechanism – the acoustic velocity attenuation depends on the distance travelled by the propagating wave and also on the sound wavelength, the good news is that is not depends on the rms acoustic particle velocity derivative that invalidated the previous mechanism. Setting the distance traveled in the order of 0,1 m the velocity ratio defined in “Eq. 10” yields:

Comunello, N.J., Martins, C.A. and Lacava, P.T.
Mixing Layer Formation Under Sound Wave Motion

$$R'_a = \frac{u'_{rms} - u'_{a rms}}{u'_{rms} + u'_{a rms}} = \frac{1 - e^{-\frac{1}{2} \left(\frac{2\pi}{\lambda}\right)^2 \frac{(\eta + \frac{4}{3}\mu)}{\rho_0 c} x}}{1 + e^{-\frac{1}{2} \left(\frac{2\pi}{\lambda}\right)^2 \frac{(\eta + \frac{4}{3}\mu)}{\rho_0 c} x}} = \begin{cases} 8 \cdot 10^{-6} \text{ for } 100 \text{ Hz} \\ 20 \cdot 10^{-6} \text{ for } 161 \text{ Hz} \end{cases}$$

The velocity ratio close to null means that there is no shear and the flow should be uniform.

Both solutions were discarded based in the analysis of the quantification proposed. Looking for a possible recycling, it was recognized the quality of the shear flow instability solution to attend the experience observations where the time to begin the mixing layer is in the same order. One possible mistake in the quantification of this mechanism could be the definition of the velocity ratio based in the rms acoustic velocity, which can hide the difference of the velocities in time due a phase shift. The rms acoustic velocity could be the same for both regions, however if they are shifted 180 degrees, the maximum velocities difference should be the double and not null, this proves by absurd that the velocity ration definition was mishandled. Besides this, it is expected that the wave propagation speed in the low and high concentration regions are slightly different due the differences in the ratios between the specific heat capacities.

Keeping the raw acoustic particle velocities, the velocity ratio of "Eq. 10" can be rewritten as:

$$R' = \frac{u'_l - u'_h}{u'_l + u'_h} \quad (13)$$

Where R' is the local acoustic velocity ratio, u'_l is the acoustic particle velocity in the low concentration region and u'_h is the acoustic particle velocity in the high concentration region.

The ratio of the acoustic particle velocity in the high concentration medium to the low concentration region, this considered without attenuation, after Morse and Ingard (1968), for a plane wave is:

$$\frac{u'_h}{u'_l} = e^{-\frac{1}{2} \left(\frac{w}{c_h}\right)^2 \frac{(\eta + \frac{4}{3}\mu)}{\rho_{0h} c} x} \cos\left(w \left(\frac{1}{c_h} - \frac{1}{c_l}\right) x\right) \quad (14)$$

Where c_h and c_l are the sound propagation speeds at the high and low oil concentration regions respectively, ρ_{0h} is the average density of the high concentration region.

Substituting "Eq. 14" in the "Eq.13" the local acoustic velocity ratio is:

$$R' = \frac{u'_l - u'_h}{u'_l + u'_h} = \frac{1 - e^{-\frac{1}{2} \left(\frac{w}{c_h}\right)^2 \frac{(\eta + \frac{4}{3}\mu)}{\rho_{0h} c} x} \cos\left(w \left(\frac{1}{c_h} - \frac{1}{c_l}\right) x\right)}{1 + e^{-\frac{1}{2} \left(\frac{w}{c_h}\right)^2 \frac{(\eta + \frac{4}{3}\mu)}{\rho_{0h} c} x} \cos\left(w \left(\frac{1}{c_h} - \frac{1}{c_l}\right) x\right)} \quad (15)$$

The cosine factor implies that the denominator of the above equation after a certain distance may range between almost 2 down to close to null, this last case when the acoustic particles at high and low concentration region are travelling in opposite directions, this leads to a very high velocity ratio, which means that there is net shear and the flow becomes unstable.

The consequence for the wave motion is that the rotational -or transverse- part of the acoustic velocity becomes important, with only happens near the boundary, in this case the null or the opposite acoustic particle velocity in the high concentration region will acts as a boundary condition. After Morse and Ingard (1968), is it foreseen that a possible solution is a shear wave, which dies out rapidly and obeys a diffusion rather than a wave equation.

7. CONCLUSIONS

For the tests inside a duct with input frequencies at 100 Hz and 161 Hz the main achievements in this work are:

- The plane sound waves can promote mixing layers inside a duct initially with high and low oil concentration regions apart.
- The mixing layer observed isn't related to the heating process caused by the sound wave energy dissipation due the viscosities.
- The mixing layers observed are likely related to the shear flow instabilities caused by the difference in the acoustic particle velocities developed in each region.
- It is suggested to perform additional tests at different input frequencies and instrumentation able to acquire the oil concentration, the acoustic pressure and particle velocity.
- It is recommended to develop the shear flow instability evaluation for oscillating velocities and to look for the rotational solution of the wave motion in the boundary of the high and low oil concentration regions.

22nd International Congress of Mechanical Engineering (COBEM 2013)
November 3-7, 2013, Ribeirão Preto, SP, Brazil

8. REFERENCES

- Appleton, J.P.; Heywood, J.B., The Effects of Imperfect Fuel-Air Mixing in a Burner on NO Formation from Nitrogen in the Air and Fuel, *Proceedings of the Combustion Institute*, 14, 777-786, 1972
- Billet, G., Giovangigli, V. and Gassowski, G., 2008, "Impact of volume viscosity on a shock/hydrogen bubble interaction". *Combustion Theory and Modelling*, vol. 12, no. 2, pp. 221-248.
- Blevins, L.G.; Gore, J.P., A Study of Radiant Tube Flame Structure and NO_x Emissions, *Combustion Science and Technology*, 109 (1-6), 255-271, 1995.
- Chapman, S. and Cowling, T.G., 1953, "The Mathematical Theory of Non-Uniform Gases", Cambridge University Press, Great Britain, 1953.
- Comunello, N.J., Martins C.A. and Lacava, P.T. , 2013. "The measurement of the acoustic particle velocities inside a rectangular duct using particle imaging velocimetry technique". In *Proceedings of the 22nd International Congress of Mechanical Engineering -COBEM2013*. Ribeirão Preto, Brazil.
- Huerre, P., 2000. "Open shear flow instabilities". *Perspectives in fluid dynamics*, Cambridge University Press, UK, pp. 159-229.
- Lyons, V.L., Fuel/Air Nonuniformity - Effect on Nitric Oxide Emissions, *AIAA Journal*, 20(5), 660-665, 1982.
- Kampen, J. F., 2006, "Acoustic pressure oscillations induced by confined turbulent premixed natural gas Flames", PhD thesis, University of Twente, Enschede, The Netherlands, p. 260.
- Morse, P.M. and Ingard, K.U., 1968, "Theoretical Acoustic", McGraw-Hill Book Company, New York, NY, USA.

9. RESPONSIBILITY NOTICE

The authors are the only responsible for the printed material included in this paper.